5-15-2007

Magnetic Behavior of Manganese-Doped ZnSe Quantum Dots

Amit D. Lad
University of Pune

Ch. Rajesh
University of Pune

Mahmud Khan
Southern Illinois University Carbondale

Naushad Ali
Southern Illinois University Carbondale

I. K. Gopalakrishnan
Bhabha Atomic Research Centre

See next page for additional authors

Published in *Journal of Applied Physics*, Vol. 101 No. 10 (2007) at doi: 10.1063/1.2733625

Magnetic behavior of manganese-doped ZnSe quantum dots

Amit D. Lad and Ch. Rajesh
Department of Physics, University of Pune, Pune 411007, India

Mahmud Khan and Naushad Ali
Department of Physics, Southern Illinois University, Carbondale, Illinois 62901

I. K. Gopalakrishnan and S. K. Kulshreshtha
Novel Materials and Structural Chemistry Division, Bhabha Atomic Research Centre, Mumbai 400085, India

Shailaja Mahamuni[a)]
Department of Physics, University of Pune, Pune 411007, India

(Received 4 October 2006; accepted 19 March 2007; published online 21 May 2007)

Magnetic properties of manganese-doped ZnSe quantum dots with the size of approximately 3.6 nm are investigated. The amount of Mn in the ZnSe quantum dots has been varied from 0.10% to 1.33%. The doping level in the quantum dots is much less than that used in the precursor. The co-ordination of Mn in the ZnSe lattice has been determined by electron paramagnetic resonance (EPR). Two different hyperfine couplings 67.3×10^{-4} and 60.9×10^{-4} cm^{-1} observed in the EPR spectrum imply that Mn atoms occupy two distinct sites; one uncoordinated (near the surface) and other having a cubic symmetric environment (nanocrystal core), respectively. Photoluminescence measurements also confirm the incorporation of Mn in ZnSe quantum dots. From the Curie-Weiss behavior of the susceptibility, the effective Mn-Mn antiferromagnetic exchange constant (J_1) has been evaluated. The spin-glass behavior is observed in 1.33% Mn-doped ZnSe quantum dots, at low temperature. Magnetic behavior at a low temperature is discussed.
 [DOI: 10.1063/1.2733625]

I. INTRODUCTION

Diluted magnetic semiconductors (DMSs) are transition metal doped semimagnetic semiconductors and are known for their intriguing magneto-optical effects due to strong *sp-d* exchange interaction between band electrons and magnetic ions. DMS materials also have great potential for spintronic devices,[1] in which spin as well as charge is exploited.

Mn-doped II-VI semiconductors are peculiar DMSs.[2] High fluorescence efficiency along with magnetic ordering makes Mn an interesting transition element dopant[3–18] in the semiconductor nanoparticles. Recently, Mn-doped ZnSe nanoparticles[3–10] received much attention since it has the potential application for luminescent as well as spintronic devices.[1] Moreover, the number of Mn ions incorporated at substitutional sites can also modify the lattice parameters as well as the band gap of semiconducting materials. Additionally, the Mn-related electron paramagnetic resonance (EPR) signal is strong[3,5,11] in the ternary compounds and has been modeled for various chemical environments. However, the large variations in magnetic properties of doped quantum dots have been reported, and the role of the synthesis route in chemically controlled magnetic effects has been identified.[19,20] Consequently, the study of magnetic properties is worthwhile in each case.

Here, we report the magnetic behavior of Mn-doped ZnSe quantum dots. The concentration of Mn is varied in ZnSe quantum dots of size as small as 3.6 nm. Paramagnetic behavior is observed for all concentration of Mn in ZnSe quantum dots. The tendency of Mn to segregate at the quantum dot surface with an increasing Mn concentration has also been observed. EPR spectroscopy is employed to distinguish various sites of Mn in the ZnSe lattice. The effective Mn-Mn exchange constant in Mn-doped ZnSe quantum dots is deduced from the magnetic susceptibility measurements.

II. EXPERIMENT

Mn-doped ZnSe quantum dots were prepared via a high temperature, organometallic synthesis route.[3] This procedure leads to highly crystalline, zinc-blende Mn-doped ZnSe quantum dots. In a typical synthesis procedure, dimethylmanganese ($MnMe_2$) was prepared by using 0.5 mL of 0.2 M manganous chloride (98%) slurry in tetrahydrofuran (THF, Qualigens) with 0.2 mL of 3 M methylmagnesium chloride in THF. The $MnMe_2$ solution was diluted with 1.8 mL of toluene (Qualigens). Part of this solution was added in 2 mL of trioctylphosphine (TOP, 90%), 1 mL of 1 M selenium (99.998%) in TOP, and 0.18 mL of 1 M diethylzinc in hexane. This organometallic precursor was injected rapidly in hexadecylamine (90%) at 300 °C. The particles were grown at 300 °C and were isolated by a standard procedure,[21] in order to obtain a fine nanocrystalline powder. All chemicals were purchased from Aldrich (unless specifically mentioned) and were used without any further purification. Undoped ZnSe quantum dots were synthesized using identical experimental conditions, excluding $MnMe_2$ in the organometallic precursor.

[a)]Electronic mail: shailaja@physics.unipune.ernet.in

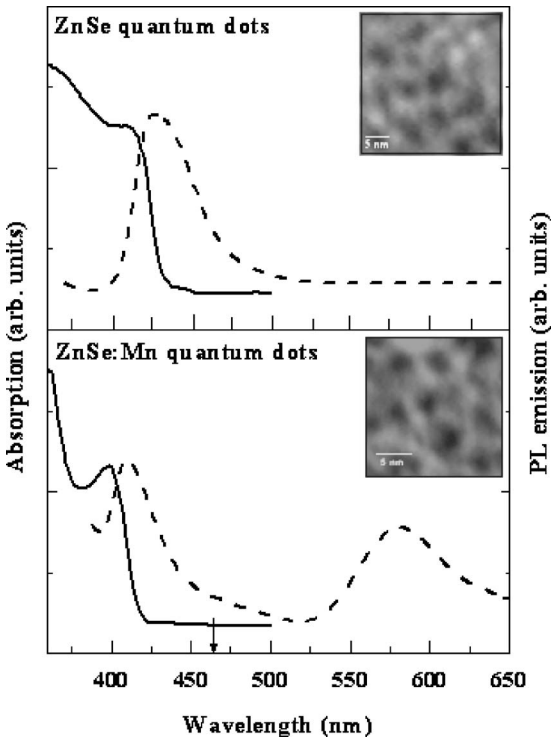

FIG. 1. Optical absorption (solid line) and photoluminescence emission (dashed line) of undoped and 0.76% Mn-doped ZnSe quantum dots. The arrow indicates the bulk band gap of ZnSe. For Mn-doped ZnSe quantum dots, the emission feature at 585 nm is attributed to the Mn $({}^4T_1 \rightarrow {}^6A_1)$ internal transition. Inset shows the TEM images of corresponding quantum dots.

Transmission electron microscopic (TEM) measurements were carried out using a Philips CM200 microscope operating at 200 kV. Optical absorption measurements were performed using a Hitachi-330, double beam spectrophotometer at room temperature. Photoluminescence was measured using an assembled photoluminescence set-up with a Jobin-Yvon 450W Xe lamp, TRIAX 180 monochromator, and photomultiplier tube. Quantitative elemental analysis of Zn, Se, and Mn of doped quantum dots was performed using inductively coupled plasma-atomic emission spectroscopy (ICP-AES) employing LABTAN-8440 Plasma Laboratory.

EPR measurements were carried out using a Bruker EMX spectrometer operating at 9.1 GHz (*X* band) microwave frequency, at liquid nitrogen temperature. Magnetic susceptibility versus the temperature curve was acquired using a superconducting quantum interference device (SQUID) magnetometer. Magnetic susceptibility measurements were performed in the temperature range of 5–400 K, in an applied magnetic field of 100 Oe. A vibrating sample magnetometer (VSM) was used to record magnetization as a function of the applied magnetic field (Model: 4500 EG and G PARC VSM).

III. RESULTS AND DISCUSSION

The crystalline phase and average size of Mn-doped ZnSe quantum dots have been determined by TEM (inset in Fig. 1). The average particle diameter for undoped ZnSe quantum dots is approximately 4.6±0.4 nm, whereas in the case of Mn-doped ZnSe quantum dots the average diameter is about 3.6±0.3 nm. The Bohr exciton diameter of bulk ZnSe (Ref. 22) as 9.0 nm, these quantum dots are in the strong confinement regime. The cubic zinc-blende ZnSe formation was checked by electron diffraction and reconfirmed by x-ray diffraction (not shown).

The quantity of Mn present in doped quantum dots has been estimated using ICP-AES measurements. The amount of Mn in ZnSe quantum dots is found to be substantially less as compared with the initial Mn concentration taken in the reaction solution (Table I). A similar observation is also reported by Suyver *et al.*[4]

Figure 1 show absorption and photoluminescence spectra of Mn-doped and undoped ZnSe quantum dots. In the case of undoped ZnSe quantum dots, the absorption feature appears at 410 nm, whereas in Mn-doped quantum dots it is blue-shifted and appears at 400 nm. The absorption spectra clearly reveal quantum size effects. Undoped ZnSe quantum dots show a blue shift in the forbidden gap by 54 nm (0.35 eV), whereas Mn-doped ZnSe quantum dots show a shift by 64 nm (0.43 eV), with respect to that of the bulk ZnSe band gap (464 nm). In the present case, it is observed that the incorporation of Mn in the ZnSe quantum dot lattice is responsible for the reduction of the growth rate. The tight binding calculations[23] predict the size of the undoped ZnSe quantum dots to be 4.3 nm, and that of the Mn-doped ZnSe quantum dots to be 3.8 nm. Moreover, the Mn-doped ZnSe quantum dots also exhibit a sharper excitionic feature at 400 nm indicating a comparatively narrow size distribution.

Evidence of successful Mn doping in ZnSe quantum dots has also been obtained from photoluminescence measurements. The photoluminescence emission (Fig. 1) of undoped as well as Mn-doped ZnSe quantum dots show strong blue emission from the lowest excited electron-hole pair, when the sample is excited with 350 nm of light. Mn-doped ZnSe quantum dots exhibit an additional orange luminescence at 585 nm, which is assigned[4] to the Mn^{2+} ${}^4T_1 \rightarrow {}^6A_1$ transition.

TABLE I. Parameters used for fitting the high temperature susceptibility data according to the Curie-Weiss law.

Concentration of Mn in percentage							
In reaction solution	ICP-AES	Calculated	$C(x)$ (10^{-6} emu/g K)	C_0 (10^{-6} emu/g K)	$\theta(x)$ (K)	θ_0 (K)	J_1 (K)
2.5	0.10	0.13	43.07	331.31	−2.4	1846.1	−28.1
5.0	0.23	0.27	89.42	331.19	−3.6	1333.3	−20.3
10.0	0.76	0.88	290.00	329.55	−7.9	897.7	−13.6
12.5	1.33	1.80	592.08	328.93	−16.0	888.8	−13.5

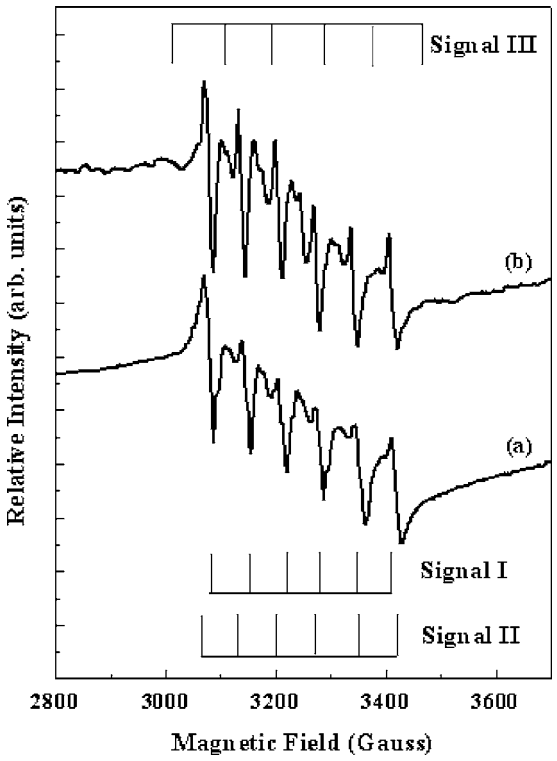

FIG. 2. EPR spectrum of (a) 0.10% and (b) 1.33% Mn-doped ZnSe quantum dots. Signal I is related to substitutional incorporation of Mn ions in ZnSe quantum dots; signal II to Mn ions located near the suface; and signal III to Mn ions bound to the surface.

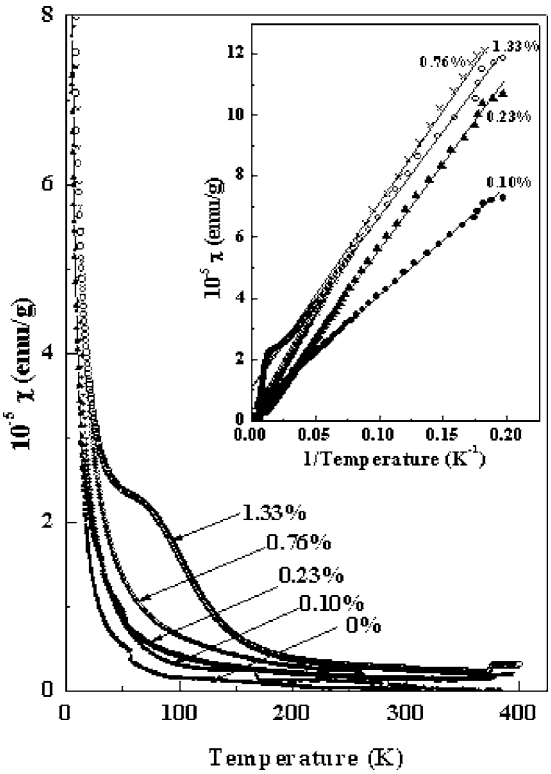

FIG. 3. Magnetic susceptibility as a function of temperature recorded by SQUID for (■) 0%, (●) 0.10%, (▲) 0.23%, (×) 0.76%, and (○) 1.33% Mn-doped ZnSe quantum dots. Inset shows magnetic susceptibility as a function of the inverse temperature for 0.10%, 0.23%, 0.76%, and 1.33% Mn -doped ZnSe quantum dots. The best fit of the high temperature data to Curie-Weiss law is shown (solid line) and fitting parameters are given in Table I.

A similar internal Mn^{2+} d-d transition ($^4T_1 \rightarrow {}^6A_1$) was also observed in Mn-doped ZnSe nanocrystals[3–8] as well as in Mn-doped ZnS nanocrystals.[12]

The crystal-field experienced by the Mn impurities will depend on the location of Mn in the host quantum dots. Also the crystal-field experienced by Mn impurities near the nanocrystal surface[11] will be significantly different from that of the bulk material. EPR measurements can give insight to the local crystal-field effects and symmetry around the Mn ions.

Figure 2(a) shows the EPR spectrum of 0.10% Mn-doped ZnSe quantum dots. Six-line hyperfine splitting is observed. The spin Hamiltonian[11,13] has been used to simulate different signals in the EPR spectrum. Two signals can be deconvoluted from the EPR spectrum. Signal I corresponds to $g=2.0024$ and hyperfine splitting constant $|A|=60.9\times10^{-4}$ cm^{-1}, whereas signal II corresponds to $g=2.0073$ and $|A|=67.3\times10^{-4}$ cm^{-1}. The value of the hyperfine splitting constant for the Mn substituted at Zn sites in the bulk ZnSe:Mn (Ref. 24) is 61.7×10^{-4} cm^{-1}. This value is close to the current experimental value for signal I, which indicates that Mn is substitutionally incorporated in the host lattice. Signal I also indicates that Mn has a cubic (T_d) symmetric environment. Moreover, at least in some of the quantum dots, the Mn-Mn interaction is strong enough to reveal the hyperfine splitting. Signal II may arise due to the location of Mn near the surface[5,11,13] of the ZnSe quantum dot. Signal II is superimposed on signal I, and is originated since Mn^{2+} has less of a symmetric environment.

For a high Mn concentration (1.33%) in ZnSe quantum dots, signal III also originates in the EPR spectrum [Fig. 2(b)], with $g=2.0069$ and $|A|=84.4\times10^{-4}$ cm^{-1}. This value of hyperfine splitting constant is related to the Mn^{2+} ions bound to the surface[13] of the ZnSe quantum dot. Mn ions bound to the surface of quantum dots show less symmetry than cubic. Thus, the hyperfine interaction is much larger than that of cubic sites. In other words, the appearance of signal III in heavily doped ZnSe quantum dots is a manifestation of segregation of Mn at the surface. Enhanced hyperfine splitting is a signature[11] of reduced covalence, and hence less coupling is anticipated between the ground state of Mn and sp-states of the nanocrystals. Less covalence might be expected for Mn located at or near the surface. The increase in the doping concentration further leads to a broad, single-line EPR signal (not shown here) which could have its origin due to the Mn pair or cluster formation.[14,25] Inevitably, aged Mn-doped ZnSe quantum dots demonstrated such a broad EPR signal.

Static susceptibility measurements also provide information about the Mn-Mn exchange interaction in DMSs. The estimation of the Mn-Mn exchange interaction is extremely important since magnetic properties of DMSs are largely governed by this interaction. The magnetic behavior of Mn-doped ZnSe quantum dots was studied using a SQUID magnetometer in the temperature range of 5–400 K. Figure 3 shows the temperature dependence of susceptibility (χ versus T) in an applied field of 100 Oe. The temperature dependent magnetic susceptibility measurements for various concentra-

tions of Mn in ZnSe quantum dots show an increase in susceptibility with a decrease in temperature. This is a typical paramagnetic behavior.

Distinct behavior is observed in heavily (1.33% Mn) doped ZnSe quantum dots. At about 165 K, magnetic susceptibility against the temperature curve indicates an onset of different mechanism. Furthermore, the magnetic susceptibility weakly depends on temperature from 65 to 46 K. The observed cusplike feature at 74 K, is attributed to characteristic of a spin-glass transition.[2,15,26] The random dispersion of Mn ions in ZnSe quantum dots may be responsible for the spin-glass type phase transition. The analogous behavior is also observed in Mn-doped CdS nanocrystals.[15] Moreover, Furdyana *et al.*[26] also observed the spin-glass transition at a low temperature (20 K) for 45% Mn-doped bulk ZnSe. Notably, in the case of quantum dots, such a spin-glass formation takes place at a much lower Mn concentration.

The calculation of χ in the high temperature ($T \geq 50$ K) regime exhibits[26] the Curie-Weiss behavior

$$\chi = \frac{C(x)}{T - \theta(x)} = \frac{C_0 x}{T + \theta_0 x}, \tag{1}$$

where

$$C(x) = \frac{(g\mu_B)^2 S(S+1)}{3k_B}\frac{N}{m}x = C_0 x,$$

N is the total number of cation sites in a sample of mass m, x is the concentration of Mn in the sample, and

$$\theta(x) = \left[\frac{2}{3}S(S+1)\sum_P J_P z_p/k_B\right]x = -\theta_0 x,$$

J_p is the exchange integral between pth neighbors and z_p is number of cations in the pth co-ordination sphere.

The Curie constant $C(x)$ and Curie-Weiss temperature $\theta(x)$ can be determined by fitting the high temperature linear part of plot χ versus $1/T$, shown in the inset of Fig. 3. The high-temperature value of χ for bulk $Zn_{1-x}Mn_xSe$ can be expressed as[26]

$$\chi = \frac{0.033x}{T + 944x}. \tag{2}$$

The effective exchange constant J_1 can be determined from θ_0 as[26]

$$\frac{J_1}{k_B} = -\frac{3}{2}\frac{\theta_0}{S(S+1)z_1}, \tag{3}$$

where $z_1 = 12$ for the zinc-blende and wurtzite DMSs, k_B is the Boltzman constant, and $S = 5/2$ for the ground state of Mn^{2+} ions. The concentration of Mn in ZnSe quantum dots has been evaluated using Eq. (2). These values are in good agreement with that of the ICP-AES measurements. It is observed that, effective Mn-Mn exchange constant J_1 (Table I) decreases with increasing concentration of Mn. J_1 approaches the bulk $ZnSe:Mn^{2+}$ value (-13.5 ± 0.95 K) (Ref. 26) at a doping level of 1.33%. A similar trend has been observed in the case of Mn-doped PbSe quantum dots[16] and Mn-doped ZnO quantum dots.[17] Quantum dots appear to reveal bulk type behavior albeit at a much lower doping level.

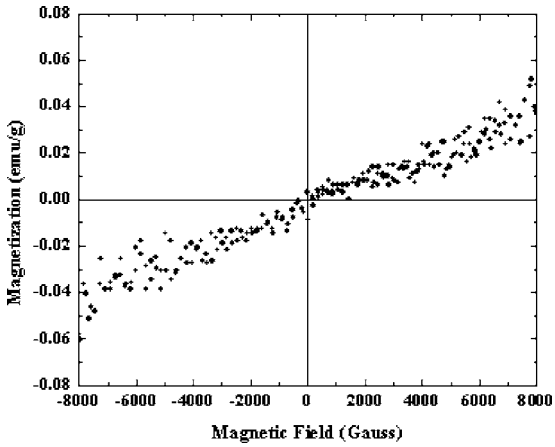

FIG. 4. Magnetization as a function of applied magnetic field reveals the paramagnetic behavior of Mn-doped ZnSe quantum dots at room temperature.

The smaller value of coupling constant in quantum dots, suggests a weak coupling between Mn spins. On the other hand, six-line splitting in the EPR data suggests that at least in some of the quantum dots Mn-Mn interaction is quite strong. Different implications for magnetic susceptibility and EPR investigations suggest that the sample may be inhomogeneous and sensitivity of Mn location may be far different in two methods.

Undoped ZnSe quantum dots are expected to be diamagnetic. However, in the present case, undoped ZnSe quantum dots indicate a paramagnetic nature. The paramagnetic behavior of undoped ZnSe quantum dots may originate due to intrinsic lattice defects. Consequently, the possibility of existence of paramagnetism in doped quantum dots due to intrinsic lattice defects cannot be ruled out. EPR studies on undoped ZnSe quantum dots show a broad signal supporting the conjecture that point defects may be present[27] in the quantum dots.

Magnetization of Mn-doped ZnSe quantum dots, as a function of the applied magnetic field has been measured for all Mn concentrations along with undoped ZnSe quantum dots, using VSM at room temperature. Figure 4 shows the linear increase of magnetization with the applied magnetic field, which also confirms the paramagnetic nature of Mn-doped ZnSe quantum dots. Undoped ZnSe quantum dots are not diamagnetic but weakly paramagnetic.

It may be noted that in the present case, the absence of ferromagnetism in Mn-doped ZnSe quantum dots can be explained with theoretical *ab initio* calculations.[28] Mn $3d$ states in the ZnSe lattice, with a cubic (T_d) crystal-field, split into an e doublet and a t_2 triplet. e levels have a lower energy than t_2 levels. t_2 levels are fully occupied leading to the absence of a hole for the coupling. It can, however, be ferromagnetic if a double exchange via the localized holes is predominant.

So far, it is not possible to make ferromagnetic Mn-doped ZnS or ZnSe quantum dots. Mn doping in III-V semiconductors is advantageous as it also introduces a hole in the semiconductor. However, solubility of Mn is limited in the case of III-V semiconductors. In the case of Mn-doped InP nanoparticles,[18] highly disordered Mn centers were found to

be responsible for the reduced hybridization with the host lattice, and hence leads to a magnetically disordered state. In the present case, an insufficient number of Mn atoms within the host lattice are hindering the formation of the magnetically ordered state. Perhaps co-doping with *p*-type impurity or controlled non-stoichiometry can lead to the magnetic ordering in Mn-doped ZnSe quantum dots.

IV. CONCLUSIONS

Mn-doped ZnSe quantum dots were obtained with varying the Mn concentration. Photoluminescence and EPR measurements confirm that Mn impurity is incorporated inside the ZnSe quantum dots. In heavily Mn-doped ZnSe quantum dots, the EPR spectum has been deconvoluted in three different signals. One with $g=2.0024$ and hyperfine splitting constant $|A|=60.9\times10^{-4}$ cm^{-1}, corresponds to a bulklike substitutional site. The second signal is due to less symmetric and near surface Mn ions with $g=2.0073$ and $|A|=67.3\times10^{-4}$ cm^{-1}. Isolated Mn on the surface of ZnSe quantum dots represents the third signal with $g=2.0069$ and $|A|=84.4\times10^{-4}$ cm^{-1}. Highly Mn-doped ZnSe quantum dots exhibit a broad, single line EPR signal due to Mn pairs or cluster formation. Magnetic susceptibility measurements reveal the paramagnetic nature for a low doping level of Mn in ZnSe quantum dots (in the temperature range of 5–400 K). From the Curie-Weiss behavior of the susceptibility, the effective Mn-Mn antiferromagnetic exchange constant (J_1) has been evaluated, which is found to be larger than the bulk value. At a higher doping concentration (1.33% Mn) ZnSe:Mn quantum dots exhibit spin-glass behavior.

ACKNOWLEDGMENTS

The authors would like to acknowledge Sophisticated Analytical Instrumental Facility, Indian Institute of Technology, Mumbai for providing TEM, ICP-AES, and EPR facilities. A.D.L. and Ch. Rajesh would like to thank the Department of Science and Technology and Indian Space Research Organization for the financial support, respectively. Help in the experiments by S. P. Patole is gratefully acknowledged. Encouragement by Dr. M. C. Uttam, Indian Space Research Organization cell, University of Pune is gratefully acknowledged.

[1] I. Zutić, J. Fabian, and S. Das Sarma, Rev. Mod. Phys. **76**, 323 (2004).
[2] J. K. Furdyna, J. Appl. Phys. **64**, R29 (1988).
[3] D. J. Norris, N. Yao, F. T. Charnock, and T. A. Kennedy, Nano Lett. **1**, 3 (2001).
[4] J. F. Suyver, S. F. Wuister, J. J. Kelly, and A. Meijerink, Phys. Chem. Chem. Phys. **2**, 5445 (2000).
[5] T. J. Norman, D. Magana, T. Wilson, C. Burns, and J. Z. Zhang, J. Phys. Chem. B **107**, 6309 (2003).
[6] L. Zu, D. J. Norris, T. A. Kennedy, S. C. Erwin, and A. L. Efros, Nano Lett. **6**, 334 (2006).
[7] S. C. Erwin, L. Zu, M. I. Haftel, T. A. Kennedy, and D. J. Norris, Nature **436**, 91 (2005).
[8] N. Pradhan, D. M. Battaglia, Y. Liu, and X. Peng, Nano Lett. **7**, 312 (2007).
[9] H. R. Heulings, X. Huang, J. Li, T. Yen, and C. L. Lin, Nano Lett. **1**, 521 (2001).
[10] E. M. Olano, C. D. Grant, T. J. Norman, E. W. Castner, and J. Z. Zhang, J. Nanosci. Nanotechnol. **5**, 1492 (2005).
[11] T. A. Kennedy, E. R. Glaser, P. B. Klein, and R. N. Bhargava, Phys. Rev. B **52**, R14356 (1995).
[12] R. N. Bhargava, D. Gallagher, X. Hong, and A. Nurmikko, Phys. Rev. Lett. **72**, 416 (1994).
[13] P. H. Borse, D. Srinivas, R. F. Shinde, S. K. Date, W. Vogel, and S. K. Kulkarni, Phys. Rev. B **60**, 8659 (1999).
[14] H. Zhou, D. M. Hofmann, H. R. Alves, and B. K. Meyer, J. Appl. Phys. **99**, 103502 (2006).
[15] N. Feltin, L. Levy, D. Ingert, E. Vincent, and M. P. Pileni, J. Appl. Phys. **87**, 1415 (2000).
[16] T. Ji, W.-B Jian, J. Fang, J. Tang, V. Golub, and L. Spinu, IEEE Trans. Magn. **39**, 2791 (2003).
[17] D. D. Sarma, R. Viswanatha, S. Sapra, A. Prakash, and M. Garcia-Hernadez, J. Nanosci. Nanotechnol. **5**, 1503 (2005).
[18] K. Somaskandon, G. M. Tsoi, L. E. Wegner, and S. L. Brock, Chem. Mater. **17**, 119 (2005).
[19] P. Crespo, R. Litran, T. C. Rojas, M. Muligner, J. M. de la Fuente, J. C. Sanchez-Lopez, M. A. Garcia, A. Hernando, S. Penades, and A. Fernandez, Phys. Rev. Lett. **93**, 087204 (2004).
[20] P. V. Radovanovic and D. R. Gamelin, Phys. Rev. Lett. **91**, 157202 (2003).
[21] M. A. Hines and P. Guyot-Sionnest, J. Phys. Chem. B **102**, 3655 (1998).
[22] A. V. Nurmikko and R. L. Gunshor, J. Lumin. **52**, 89 (1992).
[23] S. Sapra and D. D. Sarma, Phys. Rev. B **69**, 125304 (2004).
[24] G. W. Ludwing and H. H. Woodbury, *Electron Spin Resonances in Semiconductors, Solid State Physics* (Academic, New York, 1962).
[25] I. Yu and M. Senna, Appl. Phys. Lett. **66**, 424 (1995).
[26] J. K. Furdyna, N. Samarth, R. B. Frankel, and J. Spalek, Phys. Rev. B **37**, 3707 (1988).
[27] S. D. Setzler, M. Moldovan, Z. Yu, T. H. Myers, N. C. Giles, and L. E. Halliburten, Appl. Phys. Lett. **70**, 2274 (1997).
[28] X. Huang, A. Makmal, J. R. Chelikowsky, and L. Kranik, Phys. Rev. Lett. **94**, 236801 (2005).